NIST Special Publication 260-217

Certification of Standard Reference Material® 17g: Sucrose Optical Rotation

Michael A. Nelson
Brian E. Lang
Jerome Mulloor
Blaza Toman
Masaaki Ishikawa
Yoshiro Kondo

This publication is available free of charge from:
https://doi.org/10.6028/NIST.SP.260-217

National Institute of Standards and Technology
U.S. Department of Commerce

This page intentionally blank.

NIST Special Publication 260-217

Certification of Standard Reference Material® 17g: Sucrose Optical Rotation

Michael A. Nelson
Brian E. Lang
Jerome Mulloor
Chemical Sciences Division
Material Measurement Laboratory

Blaza Toman
Statistical Engineering Division
Information Technology Laboratory

Masaaki Ishikawa
Yoshiro Kondo
JASCO Corporation

This publication is available free of charge from:
https://doi.org/10.6028/NIST.SP.260-217

January 2022

U.S. Department of Commerce
Gina M. Raimondo, Secretary

National Institute of Standards and Technology
James K. Olthoff, Performing the Non-Exclusive Functions and Duties of the Under Secretary of Commerce for Standards and Technology & Director, National Institute of Standards and Technology

National Institute of Standards and Technology Special Publication 260-217
Natl. Inst. Stand. Technol. Spec. Publ. 260-217, 40 pages (January 2022)
CODEN: NSPUE2

This publication is available free of charge from:
https://doi.org/10.6028/NIST.SP.260-217

Abstract

Standard Reference Material (SRM) 17g Sucrose Optical Rotation is certified as a chemical substance of known purity. It is intended for use as a saccharimetry standard in calibrating polarimetric systems. A unit of SRM 17g consists of one bottle containing 60 g of crystalline sucrose. This publication documents the production, analytical methods, and computations involved in characterizing this product.

Keywords

Polarimetry;
Quantitative Proton Nuclear Magnetic Resonance Spectroscopy With Internal Standard;
Saccharimetry;
Specific Rotation
Standard Reference Material (SRM);
Sucrose
°Z Scale

Technical Information Contact for this SRM

Please address technical questions you may have about this SRM to srms@nist.gov where they will be assigned to the appropriate Technical Project Leader responsible for support of this material. For sales and customer service inquiries, please contact srminfo@nist.gov.

Table of Contents

List of Tables

List of Figures

Acronyms

ANOVA	analysis of variance
COA	Certificate of Analysis
FID	free induction decay
HSQC	heteronuclear single quantum correlation NMR
ICUMSA	International Commission for Uniform Methods of Sugar Analysis
IS	internal standard
KHP	potassium hydrogen phthalate
NIST	National Institute of Standards and Technology
NMR	nuclear magnetic resonance spectroscopy
$q^{1}H\text{-}NMR_{IS}$	quantitative ^{1}H NMR using an internal standard
SOP	standard operating procedures
SD	standard deviation
SI	International System of Units
SRM®	Standard Reference Material®
TCD	thermal conductivity analyzer
TGA	thermogravimetric analysis
WSO	water saturated 1-octanol

1. Introduction

Sucrose (table sugar) is a disaccharide composed of the monosaccharides glucose and fructose linked via an ether bond. Figure 1 displays its chemical structure.

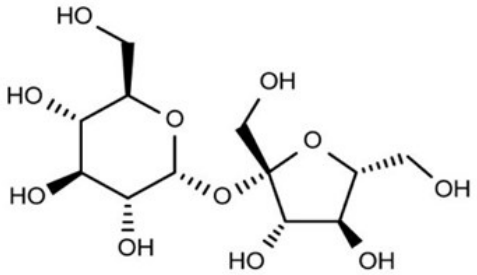

Figure 1. Chemical Structure of Sucrose, $C_{12}H_{22}O_{11}$, 342.296 g/mol

Sucrose is refined from crop plants, primarily sugar cane and beets. It is a widely traded commodity, with current world exports of raw sugar exceeding 5×10^{10} kg/year and having a market value in excess of 10^{10} $/year [1,2,3]. Exports are currently about a third of total world production [2]. Figure 2 displays estimates of export quantity and value from 1990 to 2020.

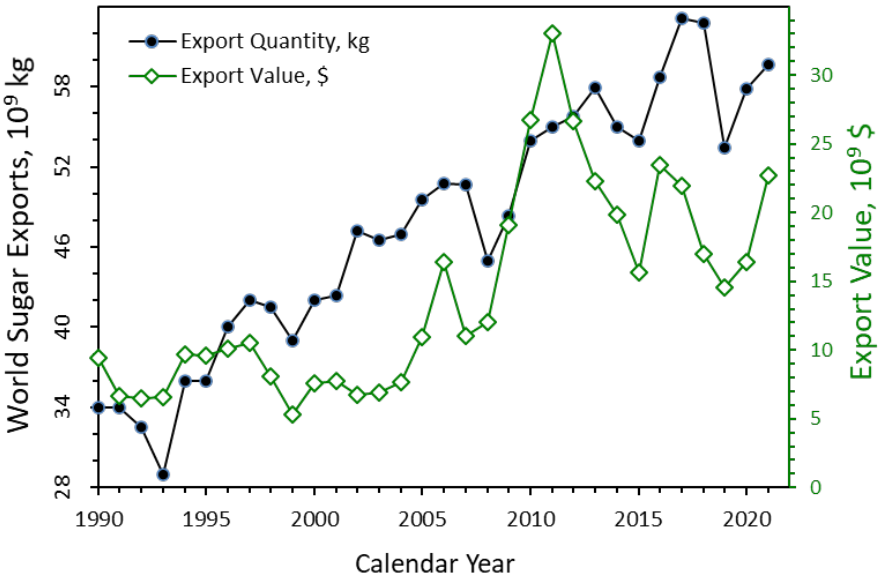

Figure 2. World Export Quantity and Value of Raw Sugar Over Time

1]; for 2018 to projection for 2021 [2]; export quantity data for 1990 to 1999 from Figure 1 of [3]. Export value not adjusted for inflation.

The U.S. Department of Agriculture's Farm Service Agency (USDA FSA) defines "raw sugar" as "any sugar not suitable for human consumption without further refinement" [4].

1.1. SRM 17 Sales History

The initial SRM 17 (Standard Sample 17 Sucrose) was issued in 1963. SRM 17g is the sixth replacement material (SRM 17b was never issued). Figure 3 displays the number of units sold as a function of time from 1990 when currently accessible sales records were created to the date of the most recent sale. Annual sales have averaged about 200 units per year.

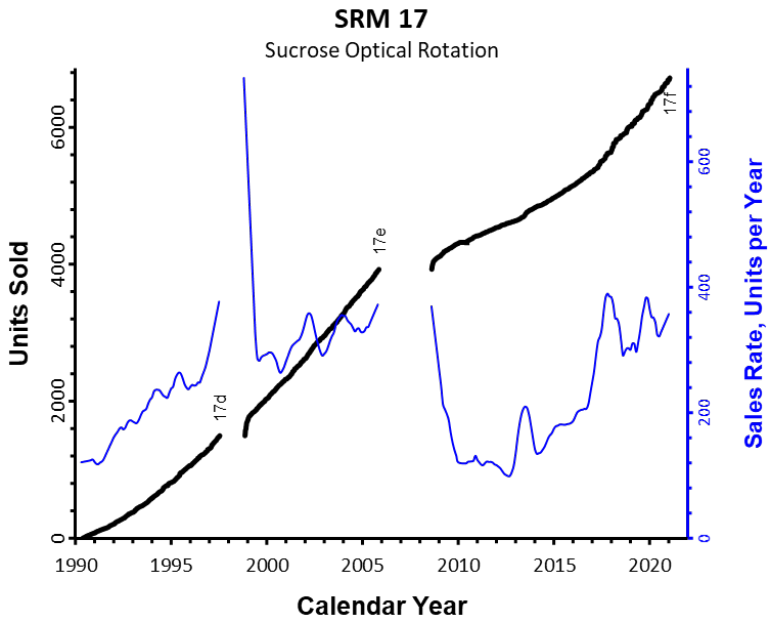

Figure 3. Sales History of SRM 17, 1990 to 2021

Figure 4 displays the proportion of sales to various countries or geographical regions over the past three decades. While more than half of the SRM 17 sales have consistently been within the USA, the proportion was largest in the 1990s. While still a minority of sales, the proportion of sales to Asian countries has steadily increased.

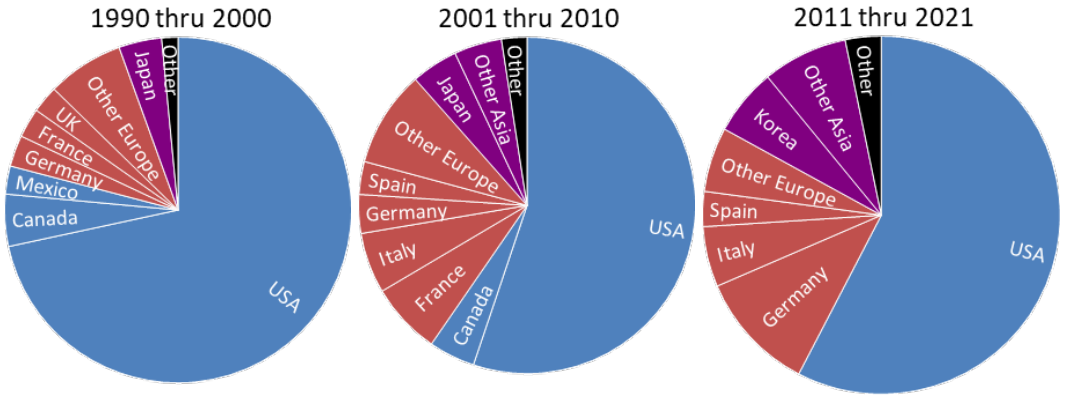

Figure 4. Location of Customers for the SRM 17 Series Materials

1.2. SRM 17's Role as an Optical Rotation Standard

Polarimetry is the measurement of the angle of rotation of linearly polarized light when passing through a sample. Polarimetric saccharimeters are instruments which measure the relationship between the optical rotation caused by an aqueous solution of a sample and that caused by a pure sucrose solution of prescribed concentration, using the same polarized light [5].

The value of raw sugar is largely determined by its sucrose content. The International Sugar Scale was defined and adopted by the International Commission for Uniform Methods of Sugar Analysis (ICUMSA) in 1932 [6,7 pp.79-80]. The scale is defined by the optical rotation of pure water and of a "normal sugar solution", where the "normal sugar solution" is defined as 26.016 0 g of "pure" sucrose weighed in vacuum, dissolved in pure water, and diluted to 100.000 cm^3 at 20.00 °C [8,9].

In practice, 100 % purity of any real substance is an unobtainable abstract ideal. However, the ICUMSA scale can be realized using sugar of suitably high purity through algebraic correction once the nature and quantity of the impurities are known. This document describes the characterization of the SRM 17g material and the confirmatory measurements which demonstrate its adequacy for use in the realization of the ICUMSA scale.

2. Material

2.1. Acquisition

350 kg of pure granular crystalline sucrose intended for production as SRM 17g Sucrose Optical Rotation were purchased from Sigma-Aldrich. Seven polymer drums, each containing 50 kg of sucrose of the same lot, were delivered to the National Institute of Standards and Technology (NIST) Gaithersburg campus on March 17, 2020 and stored in the original packaging at ambient room temperature (20 °C to 30 °C). The grain of this material is noticeably finer than that of SRM 17f Sucrose Optical Rotation [10].

2.2. Packaging

After confirmation of the material's identity and establishing that the material in all seven drums was of acceptable and acceptably consistent purity, the material was bottled, without further blending, as 60-g units in clear glass screw-cap bottles. Bottling was completed May 5, 2021. A total of 5,651 units were bottled and stored at ambient room temperature.

2.3. Identity and Suitability Assessment

Nuclear magnetic resonance (NMR) spectroscopy techniques were used to confirm chemical identity and assess whether the seven drums of the bulk sucrose were all of suitably high purity. The structure of sucrose was confirmed using ^{1}H, ^{13}C, and ^{1}H-^{13}C heteronuclear single quantum coherence (HSQC) NMR experiments. Consistency of ^{1}H NMR spectra for the bulk material and SRM 17f was demonstrated. The purity of the seven drums of the bulk material was assessed with quantitative ^{1}H NMR using an internal standard ($q^{1}H\text{-}NMR_{IS}$) [11,12,13,14,15,16].

2.3.1. Sample Preparation

For each of the seven drums, a several-gram aliquot was sampled from the top of the drum and stored in a clean glass vial. Potassium hydrogen phthalate (KHP) was used as the $q^{1}H\text{-}NMR_{IS}$ internal standard (IS); the IS source was SRM 84k Potassium Hydrogen Phthalate $KHC_8H_4O_4$ Acidimetric Primary Standard [17] with a certified mass fraction purity of (99.991 1 ± 0.005 4) %. Approximately 0.7 mL of 99.9 % D Atom purity D_2O (Cambridge Isotope Laboratories, Tewksbury, MA) was used to dilute the samples. All samples were sonicated and vortexed to achieve complete dissolution of the pure materials.

For examination of sucrose identity, a sample containing ≈10 mg of SRM 17g from bulk drum 7 in D_2O was prepared. A comparable amount of KHP was added to this sample to verify that it is suitable for use as the internal standard. A sample with a commensurate amount of SRM 17f in D_2O was prepared and analyzed to compare NMR spectra of the two sucrose materials.

Two sets of qNMR samples containing sucrose and SRM 84k KHP were prepared for the $q^{1}H\text{-}NMR_{IS}$ analyses. Both sets contained one sample from each of the seven aliquots. Sample set 1 was prepared and measured on January 7, 2021; set 2 was prepared and measured on January 11, 2021. The solutions of sucrose and KHP were observed to be stable throughout the twelve-hour period of qNMR measurements for each sample set.

Glass weigh bottles and spatulas used during sample preparation were rinsed with acetone, ethanol, methanol, and distilled water, baked in a furnace at 450 ˚C, and stored in a desiccator. Bruker 600 MHz NMR tubes (5 mm internal diameter, 17.8 cm length) were used as provided by the manufacturer. Sample mass determinations and preparation for ^{1}H NMR analysis were performed in accordance with balance use and sample preparation standard operating procedures (SOPs). Neat material masses were determined using an ultra-microbalance with 0.1 µg readability.

2.3.2. NMR Spectroscopy

Experimental NMR data were acquired using a Bruker Avance II 600 MHz spectrometer equipped with a 5-mm broadband inverse detection probe and operating with Topspin (Version 3.2) software.

2.3.2.1. Identity Confirmation

Figure 5 displays the ^{1}H NMR spectra of the SRM 17f and 17g materials. The spectra are essentially identical. The is no evidence of structurally-related impurities.

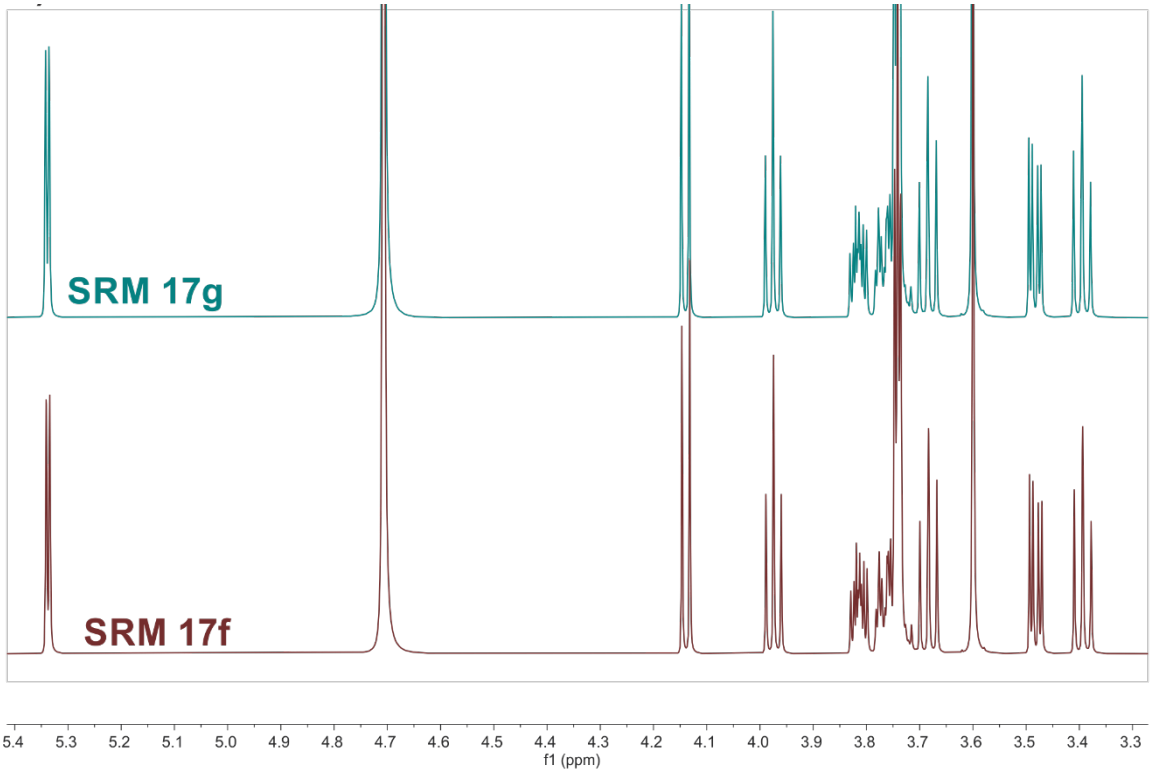

Figure 5. Comparison of ^{1}H-NMR Spectra of SRM 17f and 17g Sucrose in D_2O

Figure 6 displays the ^{1}H and ^{1}H-^{13}C HSQC NMR spectra of the SRM 17g bulk material, along with the sucrose structural assignments. The spectra are consistent with the signals expected for sucrose.

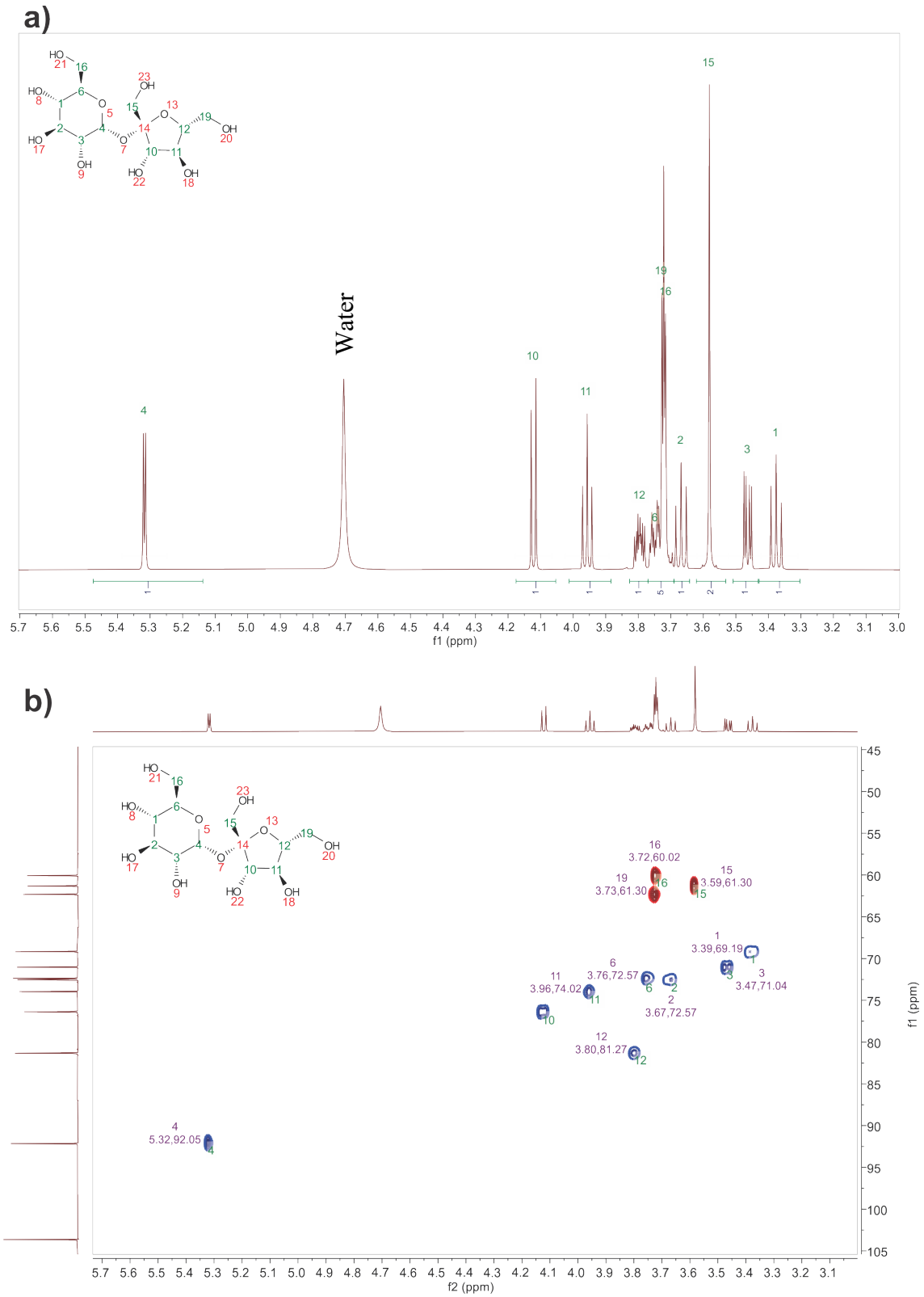

Figure 6. NMR Confirmation of Chemical Identity of Bulk SRM 17g Sucrose in D_2O
a) ^{1}H-NMR spectrum; b) ^{1}H multiplicity-edited ^{1}H-^{13}C HSQC spectrum

2.3.2.2. Suitability Assessment

The ^{1}H experimental analyses, subsequent data processing and chemical mass fraction purity determinations were performed according to the appropriate SOPs. Experiments were performed at a temperature of 298 K, the spectral sweep width was set to 20.027 6 ppm, and the transmitter frequency offset for ^{1}H was set to 6.175 ppm. 90-degree excitation pulse widths were used for these analyses and GARP Composite pulse ^{13}C decoupling was executed during free induction decay (FID) signal acquisition. Transmitter frequency offset of the carbon channel for ^{13}C decoupling experiments was 95 ppm. Data acquisition time was 4.089 446 5 s to generate an FID with 98 304 data points and 80 scans were performed for each experiment. The spin lattice relaxation time (T1) for all analyzed resonances was determined using a magnetization inversion recovery NMR experiment, with the longest T1, that of a resonance of KHP, equal to approximately 4.01 s. The recycle delay was set to 60 s, allowing for net magnetization to return to effectively 100 % of the equilibrium value prior to each pulse sequence repetition.

The purity (%), P_{P}, of a sucrose sample is determined using the following q^{1}H-NMR$_{\mathrm{IS}}$ equation [18]:

$$P_{\mathrm{P}} = \left(\frac{N_{\mathrm{I}}}{N_{\mathrm{P}}}\right) \times \left(\frac{M_{\mathrm{P}}}{M_{\mathrm{I}}}\right) \times \left(\frac{A_{\mathrm{P}}}{A_{\mathrm{I}}}\right) \times \left(\frac{m_{\mathrm{I}}}{m_{\mathrm{C}}}\right) \times P_{\mathrm{I}}, \qquad [1]$$

where N_{P} = multiplicity (# ^{1}H/peak) of the sucrose spectral peak
N_{I} = multiplicity (# ^{1}H/peak) of the KHP peak
M_{P} = relative molar mass, g/mol, of sucrose
M_{I} = relative molar mass, g/mol, of KHP
A_{P} = integrated area of the sucrose peak
A_{I} = integrated area of the KHP peak
m_{C} = mass (g) of the sampled sucrose material
m_{I} = mass (g) of the internal standard
P_{I} = mass fraction purity (%) of the internal standard

The ^{1}H multiplicities and relative molar masses (g/mol) of sucrose (N_{P}) and KHP (N_{I}) are determined by their respective chemical structures. The multiplicities are considered to be exact without uncertainty. The uncertainties of the relative molar masses are determined with a web-based molecular weight calculator [19] that applies the International Union of Pure and Applied Chemistry Guidelines provided by the Commission on Isotopic Abundances and Atomic Weights. The peak areas (A_{P} and A_{I}) are determined from the spectra, with their uncertainties estimated from the standard deviation of the respective impurity-adjusted, proton multiplicity-normalized integrals of specified resonances. The mass of the sample material and internal standard are determined by weighing, with an assigned uncertainty based on balance performance.

Table 1 lists the ^{1}H spectral regions integrated for the sucrose (A_{P}) and KHP (A_{I}). Manual phasing was performed for each spectrum and region-specific baseline correction was performed for each integral.

Table 1. ^{1}H-NMR Integration Regions for Sucrose Purity Assessment

Analyte	Chemical Shift (ppm)	Multiplet Type	Proton Moiety	Proton Multiplicity
Sucrose	5.3 4.2 to 3.3	Singlet Ten Multiplets	1,2,3,6,10,11, 12,15,16,19	1 13
Potassium Hydrogen Phthalate	7.6 to 7.5	Two Multiplets	aromatics	4

The standard uncertainty, $u(P_P)$, and the approximate 95 percent uncertainty interval about P_P was estimated using a bespoke parametric bootstrap [20] Matlab program wherein all of the above model's input variables were varied randomly. During 100 000 iterations, Gaussian kernel "pseudo values" for each of the inputs were defined using the Matlab "randn" random number generation function and each input variable's value and standard uncertainty. The value of P_P given the pseudo-value inputs was calculated and the result recorded. The uncertainties were estimated from the distribution of the 100 000 P_P results. To enable an unbiased comparison of results across the seven drums, the purity estimates were not constrained to lie between 0 g/g and 1 g/g.

Figure 7 displays the results of the q^{1}H-NMR$_{IS}$ analysis. The mean purity is adequately high. No significant bulk material heterogeneity is apparent.

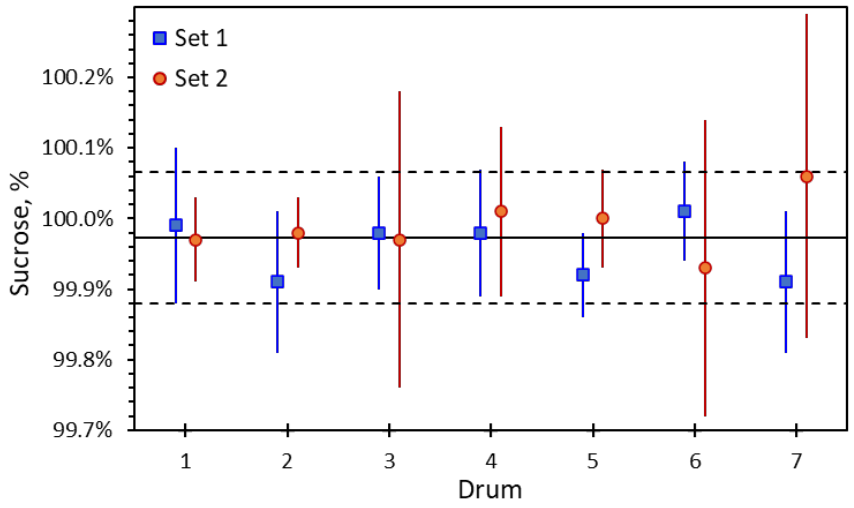

Figure 7. Purity of Bulk SRM 17g Sucrose as a Function of Drum

Symbols represent mean values; error bars represent standard deviations. Blue squares denote results from the first set of samples; red circles denote results from the second set. The solid horizontal line represents the mean of all 14 results; the dashed horizontal lines bound the approximate 95 % level of confidence interval on the distribution.

3. Microchemical Carbon and Hydrogen Analysis

Mass fractions of carbon (C) and hydrogen (H) were determined by Atlantic Microlab (Norcross, GA USA) and at NIST.

3.1. Atlantic Microlab Analysis

Three samples of the SRM 17g material were delivered to the laboratory, one each from drums 1, 2, and 6. A pure acetanilide standard, with metrological traceability to the purity value of SRM 141e Acetanilide [21], was used for quality assurance control. Samples were shipped in a cool shipping package containing approximately 2 kg of dry ice.

Elemental microanalysis was performed using sample combustion and detection of CO_2 and H_2O with thermal conductivity analyzers (TCD) to determine the C and H compositions.

3.2. NIST Analysis

Seven bottles of SRM 17g were analyzed, one from each of the barrels used in the production. SRM 350b Benzoic Acid (Acidimetric) C_6H_5COOH [22] was used as calibrant. SRM17f Sucrose Optical Rotation [10] was used as control.

A vario MACRO cube CHNOS Elemental Analyzer (Elementar Americas Inc., Ronkonkoma, NY USA) was used for the analysis. The instrument was used in the CHNS mode, using a TCD with helium as a carrier gas and oxygen to aid the combustion of the sample. The combustion tube was controlled at 1 150 °C for the analysis and the reduction tube was controlled at 950 °C. A calibrated Mettler XPR2U analytical balance was used for mass determination in the preparation of samples and standards.

Three nominal 5 mg test portions were taken from each of the seven bottles. A known mass of each test portion was added to a tared tin foil boat. After the test portion was added, the foil boat was folded and sealed to minimize entrapment of air and prevent sample loss during further handling. Three analytical samples were taken from each unit in order to achieve sufficient sampling. Samples were used as is without drying, as the material is stable and has a small water component. The control samples of SRM 17f were prepared in the same manner.

Calibration samples comprising SRM 350b were prepared by transferring a known mass of the material into tared tin foil boats of known mass. Nominal masses of SRM 350b samples having a mass range of each element that bracket the average mass of the respective element in the test samples was determined prior to preparation of calibration samples. Calibration sample masses ranged from 3 mg to 20 mg.

After enough blanks were run to ensure that blank signals for each element were sufficiently small and stable, samples were analyzed so that carryover between samples was either minimized or accounted for. Calibration samples were analyzed in order of increasing mass, followed by two blanks. The test samples were then run in a random order, beginning with a conditioning sample of the same mass to compensate for column carryover and followed by control samples. After running at least two blanks to minimize carryover, a second set of standard samples was run.

A preliminary analysis was performed for each element by fitting the calibration data to first and second order polynomials to ensure that the calibration data is fit-for-use and to remove data points suspected of being erroneous. Elemental analysis is prone to the occasional spurious data point (most likely resulting from contamination or mechanical sample loss) which is removed. Calibration points may be rejected based on analysis of the residuals of the first and second order polynomial fits. Elemental mass fractions for the analytical samples and controls are then calculated based on the first or second order polynomial fit (generally the second order polynomial is used).

After the preliminary analysis is complete, the raw data for the calibrants and test samples are exported for processing through the parametric bootstrap method. After importing the data, the best fit for the calibration data is found using an errors-in-variables model and maximum likelihood estimation. The errors-in-variables model is used to account for random effects in both the x-axis (element mass) and y-axis (detector signal). The model fits a range of polynomials to the calibration data and calculates the best polynomial degree as the one having the lowest value of the Bayesian information criterion [23]. In general, there is agreement between the results from the preliminary analysis and the bootstrap method.

Numerical analysis of the instrument data determined a consensus mass fraction of each element and its uncertainty. Uncertainty components were quantified and propagated using parametric bootstrap [20,24] and Monte Carlo [25] approaches. The uncertainty in these determinations was minimized by carefully controlled sample preparation and mass determinations, as well as an experimental design in which the sample test portions all have the same nominal mass. Small variation in the test portion masses can help minimize the uncertainty attributed to sample carryover. The two largest components of uncertainty were attributed to sample repeatability and the fit of the calibration curve.

Figure 8 displays the carbon and hydrogen elemental compositions for the seven bottles. The carbon and hydrogen results for the SRM 17f control were (42.04 ± 0.15) % and (6.485 ± 0.050) %, respectively. These are consistent with the values for carbon, (42.22 ± 0.12) %, and hydrogen, (6.47 ± 0.10) %, provided in the SRM 17f Certificate of Analysis [10]. There is no evidence of between-unit heterogeneity.

Table 2 summarizes the results of the SRM 17g analyses. The Atlantic Microlab and the NIST analyses are in excellent agreement, with the NIST results having smaller standard uncertainties. While in good agreement with the proportions expected from the molecular formula, the carbon results are slightly lower than expected while the hydrogen results are slightly higher. The differences are compatible with the presence of up to 0.1 % moisture (H_2O) in the materials as analyzed.

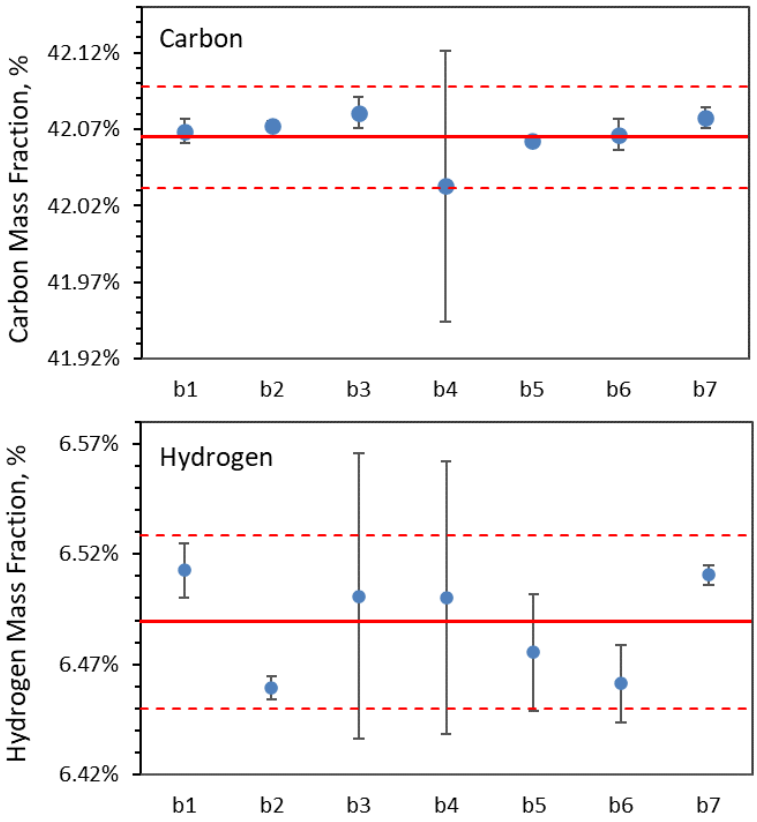

Figure 8. Elemental Compositions as Functions of Bottle Number

Each symbol represents the average mass faction for one unit; error bars represent one standard deviation. The solid horizontal line represents the consensus value as calculated by the bootstrap method. The dashed lines bound the approximate 95 % level of confidence interval on the distribution.

Table 2. Measured and Theoretical C and H Composition of SRM 17g

	Carbon [a]			Hydrogen [a]		
	x,%	*s*,%	%Δ	*x*,%	*s*,%	%Δ
Atlantic	42.078	0.061	-0.07	6.543	0.066	1.01
NIST	42.065	0.033	-0.10	6.489	0.039	0.17
Theoretical	42.106	0.002		6.478	0.001	

a *x*,% = mean of replicate analysis, expressed as % of total mass;
s,% = standard deviation of the analyses, expressed as % of total mass;
%Δ = percent bias from the theoretical composition, 100×(*x*(Measured)/*x*(Theoretical) - 1)

4. Karl Fischer Water Analysis

Seven units of candidate SRM 17g, one originating from each of the seven drums of bulk sucrose, were sampled for Karl Fischer titration moisture analysis. The bottles were selected randomly within each drum's production sequence. The reagents used in the Karl Fischer system were Hydranal composite 2 (Fluka, lot SZBD3390V), methanol (Fisher, lot 161607), and formamide (Fluka, lot SZBD2980V). Additional reagents used were one bottle of anhydrous 1-octanol obtained from Sigma-Aldrich (lot # SHBF8161V) and one bottle of LC-MS ultra chromosolve grade water obtained from Sigma-Aldrich (lot # BCBQ8032V).

The sucrose samples were analyzed without any additional treatment. The analysis was made using a volumetric Karl Fischer system with Hydranal composite 2 as the Karl Fischer reagent. The working solvent for the titration is a 1:1 (vol:vol) mixture of methanol and formamide. The Karl Fischer cell has a water jacket so that the temperature of the solution may be adjusted using an external water bath. The temperature of the water bath was set to 40 °C to aid in the dissolution of sucrose in the methanol:formamide solvent. Approximately 80 ml of the working solvent was added to the Karl Fischer vessel. The entire apparatus is enclosed in a glove bag and is purged with dry nitrogen to minimize water uptake when the solid samples are added to the Karl Fischer cell. The Karl Fischer system was run overnight to fully equilibrate.

On the day of the test measurements, the titer of the Hydranal composite 2 solution was determined from several injections of an in-house standard of water saturated 1-octanol (WSO). The WSO was prepared in 2010 and stored on the benchtop at 22 °C, where the organic phase is used for the calibration. The WSO solution is periodically checked against gravimetrically prepared water in octanol solutions, and against SRM 2890 Water Saturated 1-Octanol to confirm traceability [26]. Three to four calibration measurements using 40 mg (nominal) of WSO (or water in octanol solutions) were made by injecting the WSO into the Karl Fischer titration vessel through a silicone septum via a gas-tight syringe. Samples of the WSO were weighed out on an analytical balance that can measure down to 0.01 mg. The amount of WSO injected into the Karl Fischer cell was determined by weighing the injection syringe before and after the injection on an analytical balance.

Following the calibration measurements, two test portions of each bottle of the SRM 17g were measured. The replicates were run sequentially but the analysis order of the bottles was random. The samples were introduced into the Karl Fischer apparatus by briefly opening the fill port and adding the test portion via a glass weigh boat. The amount introduced into the Karl Fischer cell was determined with the analytical balance as the difference in mass of the weigh boat with the sample test portion and the weigh boat without it. All titrations were run for a set length of time (40 or 50 minutes, depending on the run). The drift of the instrument was calculated at the conclusion of every run over three successive 10-minute intervals to check for consistency in the baseline and to calculate the adjusted Karl Fischer signal due to system drift. After every second measurement, a blank titration was run by opening the fill port and mimicking sample introduction with the weigh boat.

The percent mass fraction of water in the sample, w_{H2O}, is calculated

$$w_{H2O} = 100\left(\frac{V_s - V_b - tR_d}{m_s}\right)F, \quad [2]$$

where: V_s volume of titrant consumed by the sucrose,
V_b volume of titrant consumed titrating a blank,
t titration time,
R_d drift rate,
m_s mass of sucrose, and
F calibration factor determined by titrating WSO samples of known water content.

The two most influential components of uncertainty were the drift rate and the determination of the calibration factor.

Figure 9 displays the measurement results for the seven bottles. The water content determined by Karl Fischer titration is (0.030 8 ±0.001 9) %, where the uncertainty represents an approximate 95 % level of confidence uncertainty on the population. There is no apparent trend in water mass fraction with respect to the fill order of the bottles. There is no significant difference in water content among the bottles evaluated.

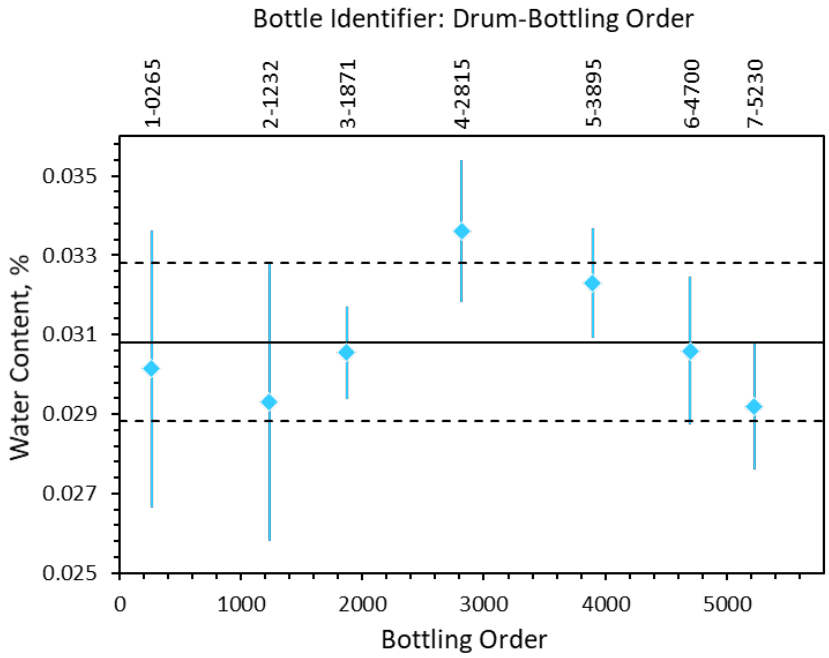

Figure 9. Water Content as a Function of Bottling Order

Each symbol represents the mean of two replicate samples from one bottle of SRM17g; error bars represent the standard deviation of two measurements. The solid horizontal line represents the mean of the seven means; the dashed lines bound the approximate 95 % level of confidence interval on the distribution.

Water content measured with mass loss on drying methods at 107 °C were consistently lower than the Karl Fischer measurements for SRM 17g and the known moisture in SRM 17f. This suggests that a significant portion of the water content is bound in the sucrose crystals.

5. Thermogravimetric Ash Analysis

Twelve bottles, at least one from each of the seven drums, were used for thermogravimetric analysis (TGA) of the non-volatile inorganic (ash) content of the SRM 17g sucrose. The bottles were selected randomly from the packaged units. Three sets of gold wires and SRM 17f served as controls.

This method is based on the gravimetric mass loss after drying in a thermogravimetric oven [27]. A test portion was removed from each bottle and heated in a LECO Thermogravimetric Analyzer 701 in an air atmosphere. The analyzer consists of an electronics unit for furnace control and data management, as well as a multiple sample furnace that allows samples to be analyzed sequentially. The furnace holds 20 crucibles and one of those crucibles is designated as an empty reference crucible. After an analysis profile was created and selected, empty crucibles were loaded into the furnace carousel and tare weights were obtained. Two runs on the TGA system were performed. The first run used test portions of 2 g taken in duplicate from each of six samples collected from the first three drums. The second run used 3 g test portions taken in duplicate from the remaining four drums and one sample from drum 2. Each crucible containing a test portion was transferred to the TGA to record an initial mass. The mass loss of each sample was monitored by the TGA and was recorded approximately every 4 min. The furnace temperature was controlled according to the selected profile. For the ash determination, the samples were heated to 107 °C and held for 4 h, heated to 300 °C and held for 1 h, heated to 500 °C and held for 1 h, then heated to 750 °C and held for 2 h. The output from the balance, a sequence of masses that changed over time, was recorded in a computer file and the data were downloaded from the instrument and analyzed off-line.

The accuracy and precision of the LECO TGA 701 instrument was monitored in real time using surrogate samples of high-purity gold wire. Three sets of gold wires (a set consisting of one large and one small gold piece) weighing a total of about 1 g were added to three different crucibles. After the initial mass of a set was recorded, the large piece of wire was removed, creating a known mass loss for that sample, which could be compared to that determined by the instrument. Any gain or loss in mass of the gold wire serves as a measure of the high temperature buoyancy correction, c_b. The difference between the room temperature mass of gold, m_{rt}, and the mass of gold at 750 °C, m_{750}, was used to determine the buoyancy correction for the thermogravimetric analyzer at 750 °C: $c_b = m_{750} - m_{rt}$.

The determinations of ash content were calculated from the final mass of the sample at 750 °C, m_f, minus the buoyancy correction, divided by the initial mass, m_i. The ash content, m_A is determined as a percent value:

$$m_A = 100\,(m_f - c_b)/m_I. \qquad [3]$$

The sources of measurement uncertainty include sample analysis repeatability, gold wire control mass determination repeatability, and weighing accuracy [27]. By far, the largest component of uncertainty in the determination of moisture in this material was sample analysis repeatability.

Figure 10 displays the measurement results for the twelve bottles. The ash content for all bottles is (0.013 2 ±0.004 0) %, where the uncertainty represents an approximate 95 % level of confidence expanded uncertainty. Given the precision of results for sample replicates, there is no apparent trend in ash content with respect to the fill order of the bottles or to bulk source drum.

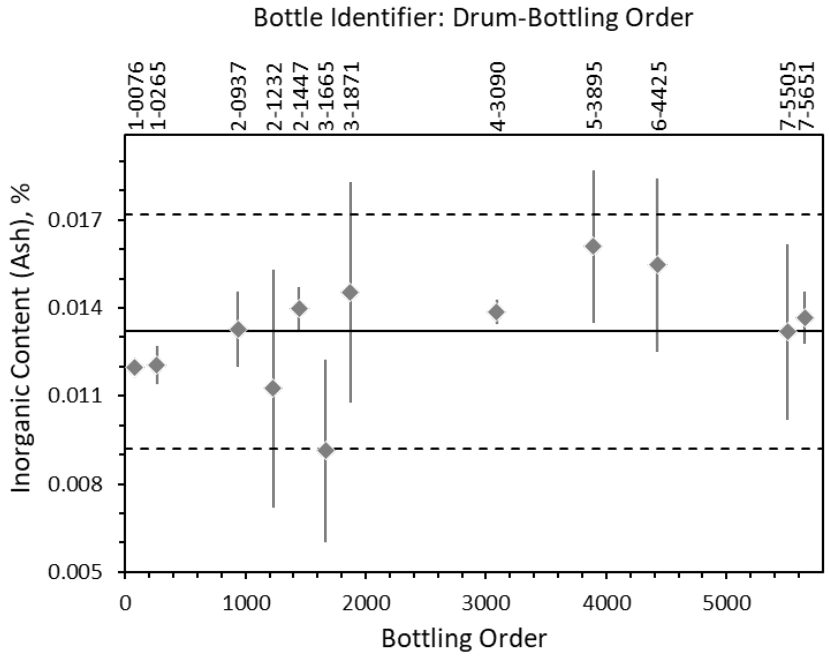

Figure 10. Non-Volatile Inorganic (Ash) Content as a Function of Bottling Order
Each symbol represents the mean of two replicate samples from one bottle of SRM17g; error bars represent the standard deviation of two measurements. The solid horizontal line represents the mean of the twelve means; the dashed lines indicate the approximate 95 % level of confidence uncertainty interval about the mean.

6. Purity Assessment

The purity of the SRM 17g sucrose after bottling was determined using the q^{1}H-NMR$_{IS}$ methods and equipment described in Section 2.3.2.2 with the following major changes:

- Samples were drawn from random samples of the bottled materials, stratified by their drum origin. Twenty-two bottles of SRM 17g were used, four from the drum 4 material and three each from the other six drums.
- Three sets of samples were prepared; two sets of seven samples and one set of eight, each on a different day so that sample processing and analysis could be reasonably managed and to minimize measurement effects due to sample lability. Samples were prepared using (10 to 15) mg subsamples from each bottle. Each sample set contained at least one bottle from each of the seven bulk drums. The three sample sets were prepared and analyzed on May 14, May 25, and June 17, 2021.
- The sucrose purity measurand, P_P, was calculated using a bespoke OpenBUGS [28] implementation of a Bayesian procedure modeled on "observation equations" [29,30]. This model groups samples from the respective bulk drums as blocks and constrains the result to lie within the interval (0 to 1) g/g. Between-drum variance is accounted for using a linear pool model to combine the purity estimates. The calculation of uncertainty includes the variation associated with the terms of the measurement function (Eq. 1), analysis of the 22 units sampled from across the production lot, and the between-drum variation.

6.1. Results

The spectral regions evaluated for sucrose and KHP are described in Table 1. Results calculated using either of the two sucrose integral regions are mutually consistent. The results reported here are based on means of ^{1}H multiplicity-normalized peak areas. Figure 11 summarizes the results of the analysis.

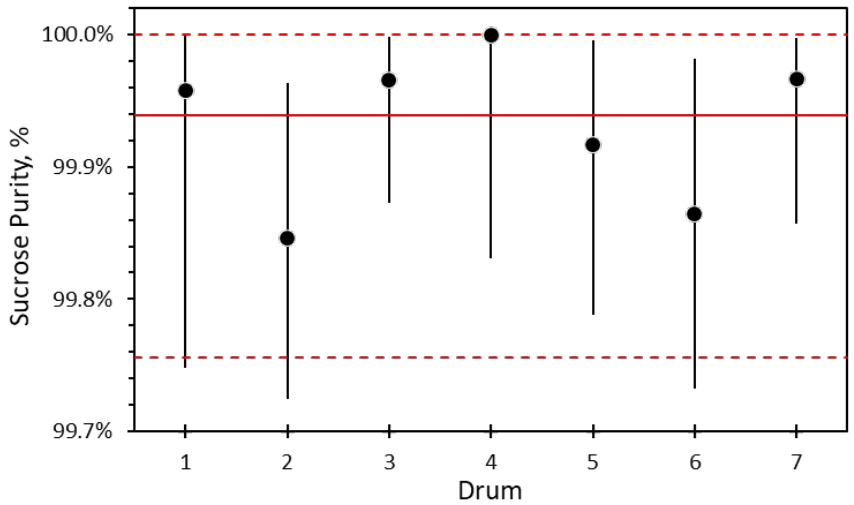

Figure 11. Purity of SRM 17g Sucrose as a Function of Drum

Each symbol represents the estimated purity result for samples from three or four SRM 17g bottles prepared from one drum of the bulk sucrose; error bars represent approximate 95 % confidence intervals. The solid horizontal line represents the median of the combined distribution; the dashed lines bound the approximate 95 % level of confidence interval on the distribution.

The purity of the SRM 17g is estimated from analysis of the posterior distribution of the OpenBUGS calculated values, shown in Figure 12.

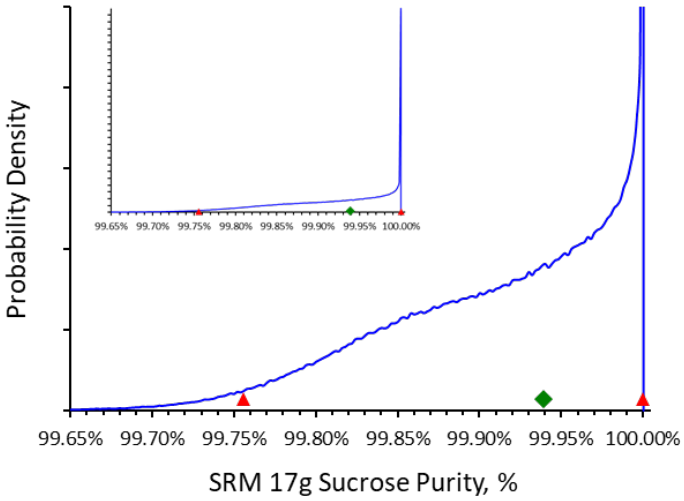

Figure 12. Posterior Distribution of SRM 17g Sucrose Purity Estimate.
The blue curve represents the distribution of the purity estimates from the OpenBUGS implementation of the Bayesian model. The red triangles indicate the lower and upper boundaries of the 95% coverage interval; the green diamond marks the median of the asymmetric distribution. The y-axis of the main plot is truncated to facilitate visualization; the inset displays the entire distribution.

The mode of the distribution at 100 % is the most probable value, however the median of the distribution provides the most representative estimate: 99.941 %. The 2.5th and 97.5th percentiles, [99.761 to 100.000] %, define a suitable 95 % level of confidence uncertainty interval about the median. While there are efficient methods for propagating this asymmetric distribution [31], for many purposes the sucrose mass fraction can be treated as following the symmetric distribution (99.88 ± 0.06) % where the ± term is a standard uncertainty associated with large degrees of freedom.

The known impurity content, (0.030 8 ±0.001 9) % moisture and (0.013 2 ±0.004 0) % ash, is (0.044 0 ±0.004 4) %, and accounts for nearly all of the difference between absolute (100 %) purity and the estimated median: 100.00 %– 99.94 % = 0.06 %.

The result is metrologically traceable to the SI unit of mass, expressed as mass fraction percent, through the verification of sucrose chemical structure and linkage of the purity value of the potassium hydrogen phthalate qNMR internal standard to that of NIST PS1 Primary Standard for qNMR (Benzoic Acid) [16,32].

6.2. Parameter Values

Table 3 lists the experimentally derived parameter values for each of the 22 samples. Table 4 lists the values for the model parameters that apply to all samples and sets.

Table 3. Per-Sample Parameter Values for Sucrose Purity Assessment

Parameter, Units	Set	$Drum_1$	$Drum_2$	$Drum_3$	$Drum_4$	$Drum_5$	$Drum_6$	$Drum_7$
A_P/N_P, area	1	1.260 083	1.420 272	1.349 543	1.301 433	1.326 072	1.240 899	1.201 256
	2	1.233 319	1.185 755	1.160 239	1.398 039	1.232 505	1.137 783	1.282 578
	3	1.265 018	1.264 463	1.651 665	1.356 861	1.222 376	1.209 349	1.324 972
	3				1.468 626			
$u(A_P/N_P)$, area	1	0.002 705	0.000 887	0.000 322	0.002 572	0.000 517	0.001 006	0.001 817
	2	0.001 430	0.002 742	0.001 224	0.001 545	0.001 252	0.001 534	0.002 918
	3	0.000 080	0.000 972	0.002 488	0.000 074	0.002 752	0.002 087	0.001 189
	3				0.003 169			
A_I/N_I, area	1	1.641 525	1.476 294	1.881 593	1.932 391	1.611 688	2.024 377	2.017 045
	2	1.990 452	2.358 281	2.187 451	3.482 349	1.671 078	2.060 668	1.652 855
	3	2.158 839	1.899 626	2.139 704	2.157 714	2.133 799	2.323 728	2.585 097
	3				2.886 062			
$u(A_I/N_I)$, area	1	0.000 121	0.000 587	0.000 714	0.000 035	0.000 791	0.000 087	0.000 070
	2	0.000 241	0.002 034	0.001 120	0.002 149	0.000 343	0.000 375	0.000 175
	3	0.001 002	0.000 590	0.001 450	0.001 035	0.001 397	0.000 040	0.000 523
	3				0.000 322			
m_C, g	1	0.010 479	0.015 430	0.011 583	0.011 561	0.013 135	0.013 018	0.010 722
	2	0.013 205	0.010 797	0.011 449	0.009 499	0.013 076	0.010 907	0.011 885
	3	0.015 156	0.011 316	0.010 480	0.008 266	0.010 883	0.009 740	0.008 436
	3				0.009 457			
m_I, g	1	0.008 151	0.009 550	0.009 632	0.010 243	0.009 516	0.012 649	0.010 738
	2	0.012 704	0.012 804	0.012 863	0.014 102	0.010 559	0.011 775	0.009 135
	3	0.015 410	0.010 131	0.008 088	0.007 837	0.011 342	0.011 151	0.009 823
	3				0.011 091			

Table 4. Sample-Independent Parameter Values for Sucrose Purity Assessment

Parameter	x	$u(x)$ [a]	unit
M_P	204.221	0.006	g/mol
M_I	342.296	0.007	g/mol
P_I [b]	0.99991	0.000 10	g/g
$u(m_C)$	Table 3	0.000 000 5	g
$u(m_i)$	Table 3	0.000 000 5	g

a OpenBUGs models parameter variability as "precision" equal to the reciprocal of the squared standard uncertainty. For example, a $u(x)$ of 0.0001 is coded as $p(x) = 1/0.000\ 1^2 = 100\ 000\ 000$.

b The certified acidimetric purity value for SRM 84k is (99.991 1 ±0.005 4) %, however the organic purity is not stated. As a conservative expedient, the number of significant digits for the parameter value used in the model has been reduced and the associated standard uncertainty enlarged.

6.3. OpenBUGS Implementation of the Model for SRM 17g Sucrose

The following is a complete OpenBUGS implementation of the model used to evaluate the SRM 17g sucrose purity.

6.3.1. Symbols Used in OpenBUGS Model

 # Inputs

AreaI 7×4 matrix of mean A_I/N_I
AreaIu 7×4 matrix of $u(A_I/N_I)$
AreaP 7×4 matrix of mean A_P/N_P
AreaPu 7×4 matrix of $u(A_P/N_P)$
avgmC 7×4 matrix of m_C
avgmI 7×4 matrix of m_I
mImCu scalar $u(m_I)$ and $u(m_C)$
N vector number of replicates per drum
#

 # Outputs

P vector mass fraction purity per drum
PLP Scalar linear pool of drum purities
#

 # Working variables

AreaIp 7×4 matrix of $p(A_I/N_I)$
AreaPp 7×4 matrix of $p(A_P/N_P)$
avgI 7×4 matrix of mean AreaI distribution (t, 2 degrees of freedom)
avgP 7×4 matrix of mean AreaP distribution (normal)
i scalar index over drums
j scalar index over replicates
KHP: scalar normal prior for the KHP internal standard
korig 7×4 matrix distribution width for avgI and avgP
k.cut 7×4 matrix non-inferential version of korig
mC 7×4 matrix normal prior for mC
mI 7×4 matrix normal prior for mI
mImCp scalar precision form of mImCu (1/variance)
mwI scalar distribution M_I (molecular weight of KHP)
mwP scalar distribution M_P (molecular weight of sucrose)
Plogit vector log-space estimate of P
PlogitLP linear pool: log-space estimate of PLP
R: vector, linear pool: Dirichlet prior for T
S vector, linear pool: shape parameters for R
T: scalar, linear pool: multinomial categorical distribution on the PlogitLP

6.3.2. OpenBUGS Model

```
Model{
KHP~dnorm(0.99991, 100000000); mImCp<-1/(mImCu*mImCu)

# calculate purity of samples from drum I, I = 1 to 7
for(i in 1:7){
  mwI[i]~dnorm(204.221, 27778); mwP[i]~dnorm(342.296, 20408)
  Plogit[i]~dnorm(5.0,0.2); P[i]<-ilogit(Plogit[i])
  for(j in 1:N[i]){
    korig[i,j]~dunif(0,0.01); k.cut[i,j]<-cut(korig[i,j])
    mI[i,j]~dnorm(avgmI[i,j],mImCp); avgI[i,j]<-KHP*mI[i,j]/(mwI[i]*korig[i,j])
    AreaIp[i,j]<-1/(AreaIu[i,j]*AreaIu[i,j]); AreaI[i,j]~dt(avgI[i,j],AreaIp[i,j],2)
    mC[i,j]~dnorm(avgmC[i,j],mImCp); avgP[i,j]<-P[i]*mC[i,j]/(mwP[i]*k.cut[i,j])
    AreaPp[i,j]<-1/(AreaPu[i,j]*AreaPu[i,j]); AreaP[i,j]~dnorm(avgP[i,j],AreaPp[i,j])}}

# Combine estimates for the seven drums using linear pool procedure
for(i in 1:7){S[i]<-1}; R[1:7]~ddirich(S[]); T~dcat(R[]); PlogitLP<-Plogit[T]; PLP<-ilogit(PlogitLP)
}
```

6.3.3. OpenBUGS Data

```
list(mImCu=0.0000005,N=c(3,3,3,4,3,3,3),

avgmI=structure(.Data=c(
  0.008151,0.012704,0.01541,NA,
  0.00955,0.012804,0.010131,NA,
  0.009632,0.012863,0.008088,NA,
  0.010243,0.014102,0.007837,0.011091,
  0.009516,0.010559,0.011342,NA,
  0.012649,0.011775,0.011151,NA,
  0.010738,0.009135,0.009823,NA),.Dim=c(7,4)),

avgmC=structure(.Data=c(
  0.010479,0.013205,0.015156,NA,
  0.015430,0.010797,0.011316,NA,
  0.011583,0.011449,0.010480,NA,
  0.011561,0.009499,0.008266,0.009457,
  0.013135,0.013076,0.010883,NA,
  0.013018,0.010907,0.009740,NA,
  0.010722,0.011885,0.008436,NA),.Dim=c(7,4)),

AreaI=structure(.Data=c(
  1.641525,1.990452,2.158839,NA,
  1.476294,2.358281,1.899626,NA,
  1.881593,2.187451,2.139704,NA,
  1.932391,3.482349,2.157714,2.886062,
  1.611688,1.671078,2.133799,NA,
  2.024377,2.060668,2.323728,NA,
  2.017045,1.652855,2.585097,NA),.Dim=c(7,4)),

AreaIu=structure(.Data=c(
  0.000121,0.000241,0.001002,NA,
  0.000587,0.002034,0.000590,NA,
  0.000714,0.001120,0.001450,NA,
  0.000035,0.002149,0.001035,0.000322,
  0.000791,0.000343,0.001397,NA,
  0.000087,0.000375,0.000040,NA,
  0.000070,0.000175,0.000523,NA),.Dim=c(7,4)),

AreaP=structure(.Data=c(
  1.260083,1.233319,1.265018,NA,
  1.420272,1.185755,1.264463,NA,
  1.349543,1.160239,1.651665,NA,
  1.301433,1.398039,1.356861,1.468626,
  1.326072,1.232505,1.222376,NA,
  1.240899,1.137783,1.209349,NA,
  1.201256,1.282578,1.324972,NA),.Dim=c(7,4)),

AreaPu=structure(.Data=c(
  0.002705,0.001430,0.000080,NA,
  0.000887,0.002742,0.000972,NA,
  0.000322,0.001224,0.002488,NA,
  0.002572,0.001545,0.000074,0.003169,
  0.000517,0.001252,0.002752,NA,
  0.001006,0.001534,0.002087,NA,
  0.001817,0.002918,0.001189,NA),.Dim=c(7,4)))
```

7. Optical Rotation Assessment

This Section describes the polarimetric assay of solutions prepared from samples of SRM 17g Sucrose Optical Rotation. This analysis was conducted to determine property values associated with the optical activity of SRM 17g and to demonstrate the fitness for purpose of SRM 17g for use in the calibration of polarimetric systems.

Seven samples from across the SRM production lot were analyzed by JASCO Corporation (Hachioji-shi, Tokyo, JP) Polarimetry laboratory, using a modern polarimeter instrument (JASCO P-2000) to measure direct light polarization through aqueous solutions of SRM 17g. Optical rotation values of light at four different wavelengths and a °Z value were determined for "normal sugar solutions" (26.016 0 g of absolutely pure sucrose per 100.000 cm^3 of otherwise pure water solution) prepared from SRM 17g, in addition to the specific rotation of SRM 17g Sucrose. The °Z scale is based upon the optical rotation for an aqueous sugar solution relative to that of a "normal sugar solution."

Measurement of optical rotation of an aqueous solution prepared from SRM 17f Sucrose was conducted to demonstrate validity of the polarimetric procedure prior to analysis of solutions prepared from SRM 17g. The measured values of optical rotation are in excellent agreement with the values provided in the Certificate of Analysis (COA) for SRM 17f [10], indicating that the calibration of the polarimeter was under adequate control and that the measurement procedure is valid.

7.1. Measurement Process

Seven units were sampled for optical rotation measurements, one originating from each of the seven drums of source material, randomly selected. Samples were numbered in accordance with the respective drum placement in the lot filling order, from Sample 1 to Sample 7. Units of SRM 17g Sucrose were stored at ambient laboratory temperature (20 to 25) °C prior to shipping and protected from direct light.

For each sample, approximately 23.70 g of sucrose was weighed under atmospheric pressure using a Mettler Toledo AX-205 Balance. The weighed sucrose samples were transferred to volumetric flasks and ultrapure water was added until the solution masses were approximately 100 g.

Optical rotation values were measured for light at λ = 546.227 1 nm (the green line of mercury isotope ^{198}Hg) and λ = 589.440 0 nm (sodium D line) through 100.02 mm pathlength of the sucrose solutions at nominal temperature of (20.00 ± 0.10) °C. The pathlength was measured via a Mitutoyo CD-S20 Caliper. Samples were analyzed in numerical order, 1 to 7 (Run 1) then repeated in reverse order, 7 to 1 (Run 2).

7.2. Calculations

An estimated value of specific rotation, expressed in (° cm^3)/(g 100 mm) , for SRM 17g Sucrose at λ = 589.440 0 nm and an estimated °Z value for light of λ = 546.227 1 nm through a "normal sugar solution" prepared from SRM 17g were calculated from blank-adjusted observed (polarimeter-indicated) values for the angle of rotation of light (optical rotation), expressed in degrees (°), through each (i = 7) of the SRM 17g sucrose solutions analyzed in

duplicate ($j = 2$), $\alpha_{observed_{i_i}}{}^{T_{i_j}}_{546.227\ 1\ \mathrm{nm}}$. Additionally, the $\alpha_{observed_{i_j}}{}^{T_{i_j}}_{546.227\ 1\ \mathrm{nm}}$ were used to calculate the angles of rotation corresponding to the °Z point and to 100 mm optical pathlengths through "normal sugar solutions" of SRM 17g for light of wavelengths λ = 589.440 0 nm, 632.991 4 nm, and 882.60 nm.

Values of specific rotation, $[\alpha]_{i_j}{}^{20.00\ °\mathrm{C}}_{\lambda}$ $\left(\frac{°\cdot \mathrm{cm}^3}{\mathrm{g}\cdot 100\ \mathrm{mm}}\right)$, for samples of SRM 17g Sucrose at λ =546.227 1 nm and λ = 589.440 0 nm wavelengths were calculated in accordance with Equation 4 using the measured $\alpha_{observed_{i_j}}{}^{T_{i_j}}_{\lambda}$ (°). For these calculations, the purity of SRM 17g was treated as practically absolute, having a value of exactly 100 %.

7.2.1. Specific rotation

Specific rotation values, $[\alpha]_{\lambda}^{20.00\ °\mathrm{C}}$, of SRM 17g at λ =546.227 1 nm and λ = 589.440 0 nm wavelengths were calculated using the measured $\alpha_{\mathrm{observed}}{}^{T}_{\lambda}$

$$[\alpha]_{i_j}{}^{20.00\ °\mathrm{C}}_{\lambda} = \frac{\alpha_{i_j}{}^{20.00\ °\mathrm{C}\prime}_{\lambda}}{l_{\mathrm{P}}\cdot C_{\mathrm{A}_i}}, \quad [4]$$

where i indexes the 7 sample solutions, j indexes the two replicate polarimetric analyses of each solution, λ is the wavelength of measurement (546.227 1 nm or 589.440 0 nm), $\alpha_{i_j}{}^{20.00\ °\mathrm{C}\prime}_{\lambda}$ is the observed angle of rotation of light at wavelength λ for the j^{th} analysis of the i^{th} solution corrected to 20.00 °C from the measured temperature, T (°C), l_{P} is the pathlength of the polarimeter cell measured via caliper (100.02 mm), and C_{A_i} is the mass concentration of the i^{th} sucrose solution.

The temperature correction is calculated

$$\alpha_{i_j}{}^{20.00\ °\mathrm{C}\prime}_{\lambda} = \alpha_{i_j}{}^{T_{i_j}}_{observed_{\lambda}}[1 - 0.000\ 37(T - 20.00\ °\mathrm{C})]. \quad [5]$$

The mass concentration of the i^{th} sucrose solution, C_{A_i} expressed in units of g/100 cm^3, is calculated

$$C_{\mathrm{A_i}} = \frac{m'_{\mathrm{S}_i}}{m'_{\mathrm{A}_i}} \times \rho_{\mathrm{A}} \times 100, \quad [6]$$

where m'_{S_i} is the mass of sucrose in the i^{th} sample solution corrected for buoyancy, m'_{A_i} is the mass of the i^{th} sample solution corrected for buoyancy, and ρ_{A} is the density of the "normal sugar solution" at 20 °C and 1 atm (1.097 631 g/cm^3).

The buoyancy corrections are accomplished using

$$m'_{\mathrm{S}_i} = m_{\mathrm{S}_i} + m_{\mathrm{S}_i} \cdot \rho^{T}_{a_{\mathrm{P}}}\left(\frac{1}{\rho_{\mathrm{S}}} + \frac{1}{\rho_{\mathrm{C}}}\right), \quad [7]$$

$$m'_{\mathrm{A}_i} = m_{\mathrm{A}_i} + m_{\mathrm{A}_i} \cdot \rho^{T}_{a_{\mathrm{P}}}\left(\frac{1}{\rho_{\mathrm{S}}} + \frac{1}{\rho_{\mathrm{C}}}\right), \quad [8]$$

where m_{S_i} is the balance indication value of the mass of sucrose in the i^{th} solution, m_{A_i} is the balance indication value of the mass in the i^{th} solution, $\rho^{T}_{a_{\mathrm{P}}}$ is the calculated density of wet air

(0.001 17 g/cm^3) at analysis laboratory temperature (24.5 °C) and atmospheric pressure (100.64 kPa), ρ_S is the density of pure crystalline sucrose (1.59 g/cm^3), and ρ_C is the density of the balance calibration weight (8.0 g/cm^3).

The density of wet air is calculated

$$\rho_{a_P}^{T} = 0.001\,293\left(\frac{273.15}{273.15+T}\right)\left(\frac{p-0.378\times e}{p_0}\right), \quad [9]$$

where T is the ambient temperature (24.5 °C), p is the atmospheric pressure (100.64 kPa), p_0 is the standard pressure of 101.325 kPa, and e is the water vapor pressure of wet air.
The water vapor pressure in wet air is calculated

$$e = 0.01(\phi)(e_0), \quad [10]$$

where ϕ is the ambient relative humidity (53.8 %), and e_0 = is the standard water vapor pressure (3.169 9 kPa).

7.2.2. International Sugar Scale, °Z

The International Commission for Uniform Methods of Sugar Analysis (ICUMSA) International Sugar Scale is used to standardize polarimetric methods of saccharimetry. The 100 °Z value of the International Sugar Scale, which ranges from 0 °Z to 100 °Z, is fixed according to the optical rotation of the green line of mercury isotope ^{198}Hg (λ = 546.227 1 nm) passing through a 200 mm length of a sugar in pure water solution, containing 26.016 0 g of (absolutely) pure sucrose, weighed in a vacuum, per 100.000 cm^3 of solution at 20.00 °C.

The value of optical rotation corresponding to the 100 °Z, $\alpha_{100\,°Z}$, is (40.777 ± 0.001) ° where the 0.001 value is a 95 % level of confidence expanded uncertainty. The 0 °Z point is fixed by the polarimeter indication of $\alpha_{546.227\,1}^{20.00\,°C}$ for 200 mm pathlength of pure water. The proportionality of values for optical rotation and sucrose concentration is linear, thus the °Z graduation is linear along the value range 0 °Z to 100 °Z.

The measured specific rotation values, $[\alpha]_{i_{j_\lambda}}^{20.00\,°C}$, were normalized to this standard scale to determine optical rotation values, $\alpha_{i_{j_{546.227\,1\,nm}}}^{20.00\,°C''}$, for l = 200 mm pathlengths of "normal sugar solutions" prepared from SRM 17g.

$$\alpha_{i_{j_\lambda}}^{20.00\,°C''} = [\alpha]_{i_{j_\lambda}}^{20.00\,°C} \times \frac{26.0160\ \text{g}}{100\ \text{mL}} \times l. \quad [11]$$

Values of $\alpha_{i_{j_\lambda}}^{20.00\,°C''}$ were also calculated for l = 100 mm pathlengths.

The value of °Z at λ = 546.227 1 nm for "normal sugar solutions" prepared from SRM 17g, °Z$_{17g}$, was determined from the $\alpha_{i_{j_\lambda}}^{20.00\,°C''}$ values for 200 mm pathlengths of the sucrose solutions. This °Z value was calculated

$$°Z_{17g} = 100\left(\alpha_{546.227\,1\,nm}^{20.00\,°C''} \Big/ \alpha_{100\,°Z}\right), \quad [12]$$

Where the value of $\alpha_{546.227\,1\text{ nm}}^{20.00\,^{\circ}\text{C}''}$ is the equally weighted mean of the mean values of $\alpha_{i\,j\,\lambda=546.227\,1\text{ nm}}^{20.00\,^{\circ}\text{C}''}$ for l = 200 mm, determined from duplicate analysis of each of the seven solutions.

7.2.3. Optical Rotation Values for Other Wavelengths

Optical rotation values for light of wavelengths λ = 589.440 0 nm, 632.991 4 nm, and 882.60 nm through 100 mm and 200 mm pathlengths were calculated

$$\frac{\alpha_{\lambda}^{20.00\,^{\circ}\text{C}''}}{\bar{\alpha}_{546.227\,1\text{ nm}}^{20.00\,^{\circ}\text{C}''}} = \frac{1}{a_0 + a_1 \cdot \lambda^2 + a_2 \cdot \lambda^4 + a_3 \cdot \lambda^6}, \qquad [13]$$

where a_0 is –0.075 047 659 000, a_1 is 3.588 221 904 585, a_2 is 0.051 946 178 300, and a_3 is –0.006 515 194 377.

7.3. Measurements and Derived Values

Table 5 lists the observed and buoyancy-corrected masses of the seven samples, m_{S} and m'_{S}, the aqueous solutions prepared from them, m_{A} and m'_{A}, and resulting sucrose concentration of the solutions, C_{A}.

Table 5. Sample Masses and Solution Masses and Concentrations

Sample (i)	Sample Mass		Solution Mass		Solution Concentration
	Observed $m_{\text{S}\,i}$, g	Corrected, $m'_{\text{S}i}$, g	Observed $m_{\text{A}\,i}$, g	Corrected, $m'_{\text{A}i}$, g	C_{A_i}, g/100 cm^3
1	23.701 86	23.722 79	100.002 80	100.124 13	25.9915 0
2	23.700 95	23.721 87	100.006 20	100.127 53	25.9896 2
3	23.702 04	23.722 97	100.004 14	100.125 47	25.9913 5
4	23.701 34	23.722 26	100.001 62	100.122 94	25.9912 4
5	23.702 07	23.723 00	99.998 54	100.119 86	25.9928 4
6	23.702 36	23.723 29	99.999 00	100.120 32	25.9930 4
7	23.701 33	23.722 25	100.001 21	100.122 53	25.9913 3

Table 6 lists the observed angle of rotation values for light passing through 100 mm of nominally "normal sugar solutions", $\alpha_{observed}{}_{\lambda}^{T}$, and the temperature-corrected angle values, $\alpha_{\lambda}^{20.00\,^{\circ}\text{C}'}$, for both replicates of the seven solutions.

Table 6. Angle of Rotation Values at λ = 546.227 1 nm and λ = 589.440 0 nm

	Sample (i)	$\alpha_{observed}{}_{i_j}{}_{\lambda}^{T_{i_j}}$				$\alpha_{i_j}{}_{\lambda}^{20.00\,°C'}$	
		$j = 1$	T_{i_1}	$j = 2$	T_{i_2}	$j = 1$	$j = 2$
λ = 546.227 1 nm	1	20.381	20.00	20.379	20.09	20.381	20.379
	2	20.382	20.04	20.379	19.93	20.382	20.378
	3	20.374	19.92	20.371	19.94	20.374	20.370
	4	20.373	19.91	20.372	19.98	20.372	20.372
	5	20.377	19.91	20.379	20.08	20.376	20.380
	6	20.383	19.98	20.381	19.98	20.383	20.380
	7	20.377	19.98	20.383	20.08	20.377	20.383
λ = 589.440 0 nm	1	17.316	20.02	17.313	20.00	17.316	17.313
	2	17.313	20.00	17.312	19.92	17.313	17.311
	3	17.310	20.03	17.306	19.94	17.310	17.306
	4	17.304	19.91	17.307	19.91	17.303	17.306
	5	17.313	19.96	17.312	19.97	17.313	17.312
	6	17.315	19.93	17.312	19.92	17.315	17.312
	7	17.310	19.92	17.314	19.94	17.309	17.313

Table 7 lists the measured values for specific rotation of SRM 17g, $[\alpha]_{\lambda}^{20.00\,°C}$, for light of λ = 546.227 1 nm and λ = 589.440 0 nm, calculated from the C_A in Table 5 and $\alpha_{\lambda}^{20.00\,°C'}$ in Table 6, for all of the solutions.

Table 7. Measured Values of Specific Rotation at λ = 546.227 1 nm and λ = 589.440 0 nm

Sample (i)	$[\alpha]_{i_j}{}_{\lambda=546.227\ 1\ nm}^{20.00\,°C}\left(\frac{° \cdot cm^3}{g \cdot 100\ mm}\right)$		$[\alpha]_{i_j}{}_{\lambda=589.440\ 0\ nm}^{20.00\,°C}\left(\frac{° \cdot cm^3}{g \cdot 100\ mm}\right)$	
	$j = 1$	$j = 2$	$j = 1$	$j = 2$
1	78.354	78.346	66.570	66.559
2	78.363	78.349	66.564	66.557
3	78.325	78.313	66.546	66.531
4	78.319	78.319	66.522	66.533
5	78.331	78.345	66.555	66.551
6	78.355	78.346	66.561	66.550
7	78.338	78.362	66.544	66.560

Table 8 lists the measured values for optical rotation of light of λ = 546.227 1 nm and λ = 589.440 0 nm through 100 mm pathlengths of "normal sugar solutions", $\alpha_{\lambda}^{20.00\,°C''}$, determined for each sample sucrose solution.

Table 8. Optical Rotation Measurements Through 100 mm of "Normal Sugar Solutions"

Sample (i)	$\alpha_{i_j}{}^{20.00\,°C''}_{546.2271\ nm}$		$\alpha_{i_j}{}^{20.00\,°C''}_{589.4400\ nm}$	
	$j = 1$	$j = 2$	$j = 1$	$j = 2$
1	20.385	20.383	17.319	17.316
2	20.387	20.383	17.317	17.316
3	20.377	20.374	17.313	17.309
4	20.375	20.375	17.306	17.309
5	20.379	20.382	17.315	17.314
6	20.385	20.383	17.316	17.314
7	20.380	20.387	17.312	17.316

7.4. Results

Figure 1 displays the two sets of specific rotation results listed in Table 7 as functions of sample number (assigned on the basis of the drum of raw material the bottle was produced from) and analysis order. There are consistent differences between the samples but there is no apparent trend with analysis order. The pattern of differences between the samples is similar for the two wavelengths.

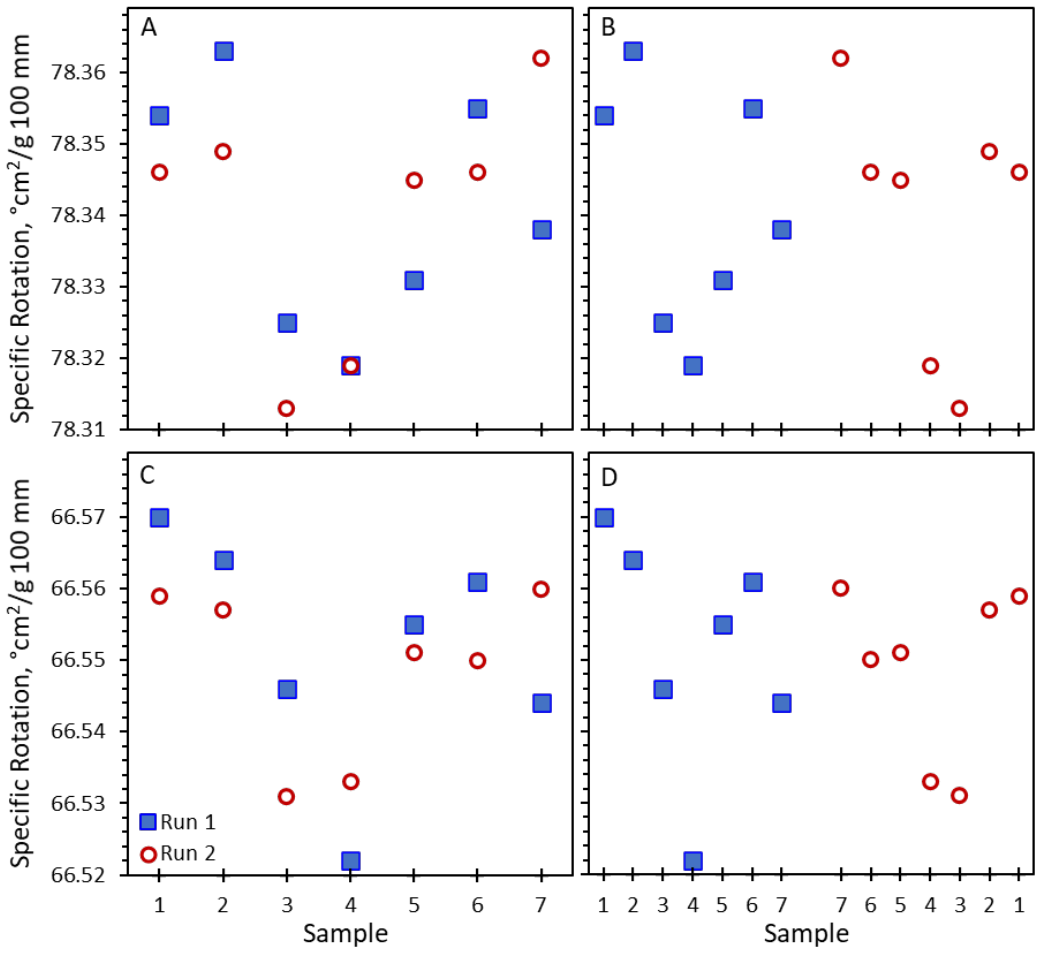

Figure 13. Measured Values of Specific Rotation at λ = 546.227 1 nm and λ = 589.440 0 nm.

Each symbol represents a measured value of specific rotation, $[\alpha]_{i_j}{}_{\lambda}^{20.00\ °C}\left(\frac{°\cdot cm^3}{g\cdot 100\ mm}\right)$, for a sample of SRM 17g. Results for Run 1 measurements (measured in order from solution i = 1 to i = 7) are shown as solid blue squares; results from Run 2 measurements (measured in order from solution i = 7 to i = 1) as open red circles. In panels A and C, the values are plotted as a function of sample number. In panels B and D, the values are plotted in the order of analysis. Panels A and B display values measured for the 546.227 1 nm wavelength; panels C and D for the 589.440 0 wavelength.

One-way analysis of variance (ANOVA) of the Table 7 results, grouped by sample number, can be used to quantify the within- and between-sample contributions to the "Type A" uncertainty in the specific rotation measurments. For balanced nested experimental designs such as used here (seven samples each analyzed twice), one-way ANOVA partitions the mean-square variance into two independent components, MS_{within} and MS_{between}. Table 9 lists the ANOVA results for the 546.227 1 nm and 589.440 0 nm values.

Table 9. One-Way ANOVA of Measured Specific Rotation Values [a]

λ	Source of Variation	*SS*	*df*	*MS*	*F*	*p*	*F*crit
546.227 1 nm	Between-sample	0.002 930	6	0.000 483 8	5.388	0.022	3.866
	Within-sample	0.000 628	7	0.000 089 8			
	Total	0.003 531	13				
589.440 0 nm	Between-sample	0.002 004	6	0.000 334 0	5.144	0.025	3.866
	Within-sample	0.000 454	7	0.000 064 9			
	Total	0.002 458	13				

a "*SS*" = Sum of Squares, "*df*" = degrees of freedom, "*MS*" = Mean Square, *F* is the *F*-statistic for the comparison, "*p*" is the probability that the observed difference between the samples could arise by chance given the magnitude of the within-sample variance, and *F*crit is the critical *F* value for the comparison.

The within- and between-sample components of measurement variance are readily calculated from the within-and between-sample mean squares (*MS*) provided by the ANOVA analysis. The within-sample variance, expressed as the square of the within-sample standard deviation, is equal to the within-sample mean square

$$s^2_{\text{within}} = MS_{\text{within}}, \quad [14]$$

The between-sample variance, expressed as the square of the between-sample standard deviation, is proportional to the difference between the between- and within-sample mean squares

$$s^2_{\text{between}} = \text{MAX}\left(\frac{MS_{\text{between}} - MS_{\text{within}}}{n_r}, 0\right), \quad [15]$$

where n_r is the number of measurements per group (here, 2) and MAX is the function "take the maximum of the series of values." The standard uncertainty of the measurement mean combines the two components

$$u_{\text{TypeA}}\left([\alpha]_\lambda^{20.00\,^\circ\text{C}}\right) = \sqrt{n_r s^2_{\text{between}} + s^2_{\text{within}}}\,. \quad [16]$$

where u_{TypeA} symbolizes the Type A components of uncertainty.

Table 10 lists the equally weighted mean of the measured specific rotation values, $[\alpha]_\lambda^{20.00\,^\circ\text{C}}$ for λ of 546.227 1 nm and 589.440 0 nm, and the estimated Type A measurement uncertainty components. The magnitudes of the components are quite similar for the two wavelengths. The between-sample variability is greater than the within-sample, suggesting that the preparation and handling of sample solutions is the largest source of variation in these data sets.

Table 10. Components of the Specific Rotation Measurement Uncertainty

	(° cm^3)/(g 100mm)				$100\,\frac{u_{\text{TypeA}}\left([\alpha]_\lambda^{20.00\,^\circ\text{C}}\right)}{[\alpha]_\lambda^{20.00\,^\circ\text{C}}}$
λ	$[\alpha]_\lambda^{20.00\,^\circ\text{C}}$	s_{within}	s_{between}	$u_{\text{TypeA}}\left([\alpha]_\lambda^{20.00\,^\circ\text{C}}\right)$	
546.227 1 nm	78.340 4	0.009 5	0.014 0	0.022	0.028 %
589.440 0 nm	66.550 2	0.008 1	0.011 6	0.018	0.027 %

The relative measurement uncertainties, $100\,\frac{u_{\text{TypeA}}([\alpha]_{\lambda}^{20.00\,^{\circ}\text{C}})}{[\alpha]_{\lambda}^{20.00\,^{\circ}\text{C}}}$, for these measurements are less than 0.03 %. This represents the repeatability precision (measurements made using the same equipment over a relatively short period) of the polarimetric procedure used. To account for between-laboratory biases attributable to the substance density values, atmospheric pressure, calibration of the polarimeter, measured pathlength of the polarimeter cell, and individual mass and temperature determinations, the Type A uncertainty is combined with an experience-based Type B relative uncertainty of 0.1 %. The combined relative standard uncertainty is $\sqrt{0.03^2 + 0.1^2} = 0.104$ % [31].

A calculated estimate of $[\alpha]_{\lambda=589.440\,0\text{ nm}}^{20.00\,^{\circ}\text{C}}$, based on the calculated values of $\alpha_{589.440\,0\text{ nm}}^{20.00\,^{\circ}\text{C}\prime\prime}$ in Table 8, is (66.522 ± 0.069) (° cm^3)/(g 100mm). The associated uncertainty was calculated similarly to that for the measured value of $[\alpha]_{\lambda=589.440\,0\text{ nm}}^{20.00\,^{\circ}\text{C}}$, except that the relative $u_{\text{Type A}}([\alpha]_{\lambda=546.227\,1\text{ nm}}^{20.00\,^{\circ}\text{C}})$ was included in the calculation of relative $u([\alpha]_{\lambda=589.440\,0\text{ nm}}^{20.00\,^{\circ}\text{C}})$ instead of the relative $u_{\text{Type A}}([\alpha]_{\lambda=589.440\,0\text{ nm}}^{20.00\,^{\circ}\text{C}})$. The calculated and measured values are consistent.

Table 11 lists $\alpha_{546.227\,1\text{ nm}}^{20.00\,^{\circ}\text{C}\prime\prime}$ and $\alpha_{589.440\,0\text{ nm}}^{20.00\,^{\circ}\text{C}\prime\prime}$ values calculated for 100 mm and 200 mm solution pathlengths. The standard uncertainties of these estimates were calculated as the relative $u_{\text{Type A}}([\alpha]_{\lambda=546.227\,1\text{ nm}}^{20.00\,^{\circ}\text{C}})$ combined with a Type B relative standard uncertainty of 0.1 %. The values are expressed both in degrees and milli-radians, where 1 plane angle degree is equal to 0.017 453 3 radians.

Table 11. Measured Values for $\alpha_{\lambda}^{20.00\,^{\circ}\text{C}\prime\prime}$ with 100 mm and 200 mm Pathlengths

	$\alpha_{\lambda}^{20.00\,^{\circ}\text{C}\prime\prime}$, $l = 100$ mm		$\alpha_{\lambda}^{20.00\,^{\circ}\text{C}\prime\prime}$, $l = 200$ mm	
λ, nm	°	mrad	°	mrad
546.227 1	20.381 ± 0.021	355.71 ± 0.37	40.762 ± 0.042	711.42 ± 0.74
589.440 0	17.314 ± 0.018	302.18 ± 0.31	34.627 ± 0.035	604.36 ± 0.61

Table 12 lists optical rotation values, $\alpha_{\text{calc}\lambda}^{20.00\,^{\circ}\text{C}\prime\prime}$, for light of wavelengths 589.440 0 nm, 632.991 4 nm, and 882.60 nm through 100 mm and 200 mm pathlengths, calculated via Equation 13 using the $\alpha_{546.227\,1\text{ nm}}^{20.00\,^{\circ}\text{C}\prime\prime}$ value. The standard uncertainties of these estimates were calculated as the relative $u_{\text{Type A}}([\alpha]_{\lambda=546.227\,1\text{ nm}}^{20.00\,^{\circ}\text{C}})$ combined with a Type B relative standard uncertainty of 0.1 %. The values are expressed both in degrees and milli-radians, where 1 plane angle degree is equal to 0.017 453 3 radians.

Table 12. Values for $\alpha_{\mathrm{calc}_\lambda}^{20.00\,^{\circ}\mathrm{C}''}$ with 100 mm and 200 mm Pathlengths

	$\alpha_{\mathrm{calc}_\lambda}^{20.00\,^{\circ}\mathrm{C}''}$, $l = 100$ mm		$\alpha_{\mathrm{calc}_\lambda}^{20.00\,^{\circ}\mathrm{C}''}$, $l = 200$ mm	
λ	°	mrad	°	mrad
589.440 0	17.306 ± 0.018	302.05 ± 0.31	34.613 ± 0.036	604.10 ± 0.62
632.991 4	14.870 ± 0.015	259.53 ± 0.27	29.740 ± 0.031	519.07 ± 0.52
882.60	7.415 ± 0.008	129.42 ± 0.13	14.830 ± 0.015	258.84 ± 0.27

From Equation 12 and the definition of $\alpha_{100\,^{\circ}\mathrm{Z}}$, the °Z value of an aqueous solution containing pure water and 26.0160 g of SRM 17g per 100 cm^3 of solution is $\alpha_{546,2271\,\mathrm{nm}}^{20.00\,^{\circ}\mathrm{C}''}/\alpha_{100\,^{\circ}\mathrm{Z}} = 100\,(40.761 \pm 0.042)/(40.777 \pm 0.001/2)$ = (99.961 ± 0.104) °Z where all of the ± values are standard uncertainties.[31].

Note: The 0.1 % Type B relative standard uncertainty component of the total combined standard uncertainties provided for the above quantities, *u*(*X*), is associated with "large" (>60) degrees of freedom. Because the Type B component is very much larger than the Type A components, the combined uncertainties are also associated with "large" degrees of freedom. Therefore, approximate 95 % level of confidence expanded uncertainties, $U_{95\%}(X)$, can be estimated as twice the combined uncertainty [31]

$$U_{95\%}(X) = 2u(X)\,. \qquad [17]$$

The measured values of optical rotation normalized to the ICUMSA International Sugar Scale are metrologically traceable to the angle of rotation of light, having wavelength of 546.227 1 nm, passing through 200 mm of a "normal sugar solution" of pure sucrose in pure water, specified as having a mass concentration, c = 26.016 0 g/100 cm^3. The specific rotation value determined for SRM 17g is metrologically traceable to the SI units of angle (rad), length (m), and mass (g) through gravimetric procedures for the preparation of sample aqueous sucrose solutions, calibration of the polarimetric measurement apparatus and balance, and adequate control of measurement conditions, including temperature, light source frequency and atmospheric pressure.

8. Acknowledgements

The authors thank Carolyn Vallone of the NIST Office of Reference Materials for providing the 1990 thru 2002 sales history of SRMs 17d and 17e, Wayne Kottkamp of JASCO Inc. (Easton, MD) for facilitation of sample delivery and polarimetric assay of SRM 17g, and JASCO Corporation for provision of results of the polarimetric assay of SRM 17g.

9. References

1 US Department of Agriculture; Foreign Agricultural Service; Production, Supply, and Distribution database; https://www.ers.usda.gov/data-products/sugar-and-sweeteners-yearbook-tables/

2 US Department of Agriculture; Foreign Agricultural Service; May 25, 2021: Sugar: World Markets and Trade. Available through https://www.fas.usda.gov/data/sugar-world-markets-and-trade

3 Mitchell D, Sugar Policies: Opportunity for Change. World Bank Policy Research Working Paper 3222 (2004) http://hdl.handle.net/10986/14307

4 USDA FSA. USDA's Domestic Sugar Program and Reporting Glossary Terms https://www.fsa.usda.gov/Internet/FSA_File/sugar_glossary.pdf (accessed 9/10/2021)

5 OIML R 14. Polarimetric saccharimeters graduated in accordance with the ICUMSA International Sugar Scale. International Organization of Legal Metrology (1995). https://www.oiml.org/en/files/pdf_r/r014-e95.pdf

6 Proceedings of the Eighth Session, International Commission for Uniform Methods of Sugar Analysis, Amsterdam, 1932. Int Sugar J 1933;35(17):62

7 Bates FJ. Circular of the Bureau of Standards no. 440: polarimetry, saccharimetry and the sugars. National Bureau of Standards Circular 440. 1942. https://doi.org/10.6028/NBS.CIRC.440

8 ICUMSA – Methods Book, Method GS2/3-1; The Braunschweig Method for the Polarization of White Sugar by Polarimetry; Bartens: Berlin, Germany (2011). https://www.bartens.com/product/2209/

9 ICUMSA Proceedings 1998, 22nd Session; Bartens: Berlin, Germany; p. 209 (1998). https://bartens.com/product/2017/

10 National Institute of Standards and Technology, Certificate of Analysis, Standard Reference Material 17f Sucrose Optical Rotation. 2013. https://www-s.nist.gov/srmors/quickSearch.cfm?srm=17f&go=Go

11 Malz F, Jancke HJ. Validation of quantitative NMR. J Pharm Biomed Anal 2005;38(5):813−823. https://doi.org/10.1016/j.jpba.2005.01.043

12 Jancke HJ, Malz F, Haesselbarth W. Structure analytical methods for quantitative reference applications. Accred Qual Assur 2005;10:421−429. https://doi.org/10.1007/s00769-005-0004-9

13 Holzgrabe U, Deubner R, Schollmayer C, Waibel B. Quantitative NMR spectroscopy – Applications in drug analysis. J Pharm Biomed Anal 2005;38(5):806−812. https://doi.org/10.1016/j.jpba.2005.01.050

14 Saito T, Ihara T, Koike M, Kinugasa S, Fujimine Y, Nose K, Hirai T. A new traceability scheme for the development of international system-traceable persistent organic pollutant reference materials by quantitative nuclear magnetic resonance. Accred Qual Assur 2009;14:79−86. https://doi.org/10.1007/s00769-008-0461-z

15 Pauli GF, Jaki BU, Lankin DC. Quantitative ^{1}H NMR: Development and Potential of a Method for Natural Products Analysis. J Nat Prod 2005;68(1):133-149. https://doi.org/10.1021/np0497301

16 Nelson MA, Waters JF, Toman B, Lang BE, Rück A, Breitruck K, Obkircher M, Windust A, Lippa KA. A New Realization of SI for Organic Chemical Measurement: NIST PS1 Primary Standard for Quantitative NMR (Benzoic Acid). Anal Chem 2018;90:10510-10517. https://doi.org/10.1021/acs.analchem.8b02575

17 National Institute of Standards and Technology, Certificate of Analysis, Standard Reference Material 84k Potassium Hydrogen Phthalate $KHC_8H_4O_4$ Acidimetric Primary Standard. 2005. https://www-s.nist.gov/srmors/certificates/archives/84k.pdf

18 Al-Deen TS, Hibbert DB, Hook JM, Wells RJ. An uncertainty budget for the determination of the purity of glyphosate by quantitative nuclear magnetic resonance (QNMR) spectroscopy. Accred Qual Assur 2004;9:55–63. https://doi.org/10.1007/s00769-003-0737-2

19 International Union of Pure and Applied Chemistry, Inorganic Chemistry Division, Commission on Isotopic Abundances and Atomic Weights. Molecular Weight Calculator. Project No. 2015-037-2-200. https://ciaaw.shinyapps.io/calculator/ (accessed 9/2/2021)

20 Efron B, Tibshirani RJ. (1993) An Introduction to the Bootstrap, Chapman & Hall, UK.

21 National Institute of Standards, Certificate of Analysis, Standard Reference Material 141e Acetanilide. 2017. https://www-s.nist.gov/srmors/view_detail.cfm?srm=141e

22 National Institute of Standards and Technology, Certificate of Analysis, Standard Reference Material 350b Benzoic Acid (Acidimetric) C6H5COOH. 2015. https://www-s.nist.gov/srmors/view_detail.cfm?srm=350b

23 Schwarz G. Estimating the Dimension of a Model. Ann Statist 1978;6(2):461-464. https://doi.org/10.1214/aos/1176344136

24 Possolo A, Pintar AL. Plurality of Type A evaluations of uncertainty. Metrologia 2017;54:617-632. https://doi.org/10.1088/1681-7575/aa7e4a

25 JCGM 101:2008; Evaluation of Measurement Data — Supplement 1 to the "Guide to the Expression of Uncertainty in Measurement" – Propagation of distributions using a Monte Carlo method, Joint Committee for Guides in Metrology (JCGM), 2008. https://www.bipm.org/en/publications/guides

26 Lang BE. Solubility of Water in Octan-1-ol from (275 to 369) K, J Chem Eng Data 2012;57(8):2221−2226. https://doi.org/10.1021/je3001427

27 Mann JL, Kelly WR, MacDonald BS. Observations of Anomalous Mass-Loss Behavior in SRM Coals and Cokes on Drying. Anal Chem 2002:74(15):3585-3591. https://doi.org/10.1021/ac0157223

28 OpenBUGS Home Page. http://www.openbugs.net/w/FrontPage
See also: Lunn D, Spiegelhalter D, Thomas A, Best N. The BUGS project: Evolution, critique and future directions (with discussion), Stat Med 2009;28:3049-3082. https://doi.org/10.1002/sim.3680

29 Toman B, Nelson MA, Lippa KA. Chemical purity using quantitative ^{1}H-nuclear magnetic resonance: a hierarchical Bayesian approach for traceable calibrations. Metrologia 2016;53,1193-1203. https://doi.org/10.1088/0026-1394/53/5/1193

30 Nelson MA, Brown Thomas J, Lang BE, Mulloor J, Sieber JR, Toman B, Yu LL, Lo S (2021) Certification of Standard Reference Material 916b: Bilirubin. NIST Special Publication (SP) 260-212. https://doi.org/10.6028/NIST.SP.260-212

31 Possolo A. Evaluating, Expressing, and Propagating Measurement Uncertainty for NIST Reference Materials. NIST Special Publication (NIST SP) 260-202 (2020). https://doi.org/10.6028/NIST.SP.260-202

32 NIST PS1 Primary Standard for quantitative NMR (Benzoic Acid), Certificate of Analysis. Date of Issue: 1 January 2018. https://www.nist.gov/document/certificate-analysis